Status of the Muon $(g - 2)$ Experiment

B. Lee Roberts
for the Muon $(g - 2)$ Collaboration [1]
Department of Physics
Boston University, Boston, Massachusetts 02215

1 Introduction

The study of g-factors of subatomic particles can trace its roots back to the 1921 paper by Stern [2], which was a proposal to study space quantization with an apparatus which is now called a "Stern-Gerlach apparatus". By 1924, the famous experiments had been done [3] and a review paper was written summarizing their results [4]. Their final conclusion, that "to within 10% the magnetic moment of the electron was one Bohr magneton", meant in modern language that the g-value of the electron was 2, where the gyromagnetic ratio g is the proportionality constant between the magnetic moment and the spin,

$$\vec{\mu} = g(\frac{e}{2m})\vec{s}. \tag{1}$$

The discovery that $g_e \neq 2$ [5], and the calculation by Schwinger [6] predicting that (to first order) the radiative correction to g_e was α/π, were important early steps in the development of Quantum Electrodynamics (see Fig. 1).

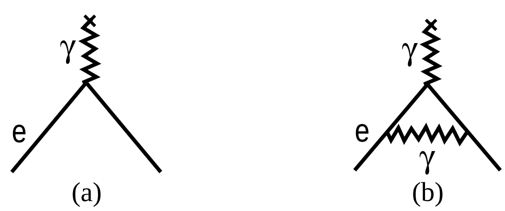

Figure 1: The Feynman graphs for $g = 2$ and the lowest order radiative correction (Schwinger term).

The long lifetime of the muon permits a precision measurement of its anomalous moment at the parts per million (ppm) level. The muon magnetic moment is given by [7]

$$\mu_\mu = (1 + a_\mu)\frac{e\hbar}{2m_\mu} \qquad \text{where} \qquad a_\mu = \frac{(g-2)}{2}. \tag{2}$$

The electron anomalous magnetic moment has been measured to a few parts per billion (ppb) [8], and can be completely described by QED of electrons and photons to eighth order, $(\frac{\alpha}{\pi})^4$. The contributions of virtual muons, tauons, etc., enter at the few ppb level. The calculation of the electron anomalous moment is limited by the knowledge of the fine-structure constant. With the reliability of modern QED calculations, Kinoshita has turned things around and has used the electron g value measurement to give the best value for α [9].

The relative contribution of heavier particles to the muon anomaly scales as $(m_\mu/m_e)^2$ and the famous CERN experiment [10], which obtained a relative error on a_μ of $\pm$ 7.3 ppm, easily observed the predicted $\sim$ 60 ppm contribution of virtual hadrons.

In 1984, efforts began to make a new measurement of the muon anomalous moment to a precision of ± 0.35 ppm, which would represent a 5 standard deviation observation of the electroweak contribution, and would also be sensitive to contributions from "new physics" such as muon substructure or supersymmetry.

2 Theoretical Contributions to $(g-2)$

The Standard Model value of a_μ is given by $a_\mu(\mathrm{SM}) = a_\mu(\mathrm{QED}) + a_\mu(\mathrm{hadronic}) + a_\mu(\mathrm{weak})$, and any contribution from new physics would be reflected in a measured value which did not agree with the Standard Model.

Comparison of the measurements and calculations of the electron g value gives one great confidence in our understanding of QED [9] to the level needed for muon $(g-2)$. Taking the value of α from the electron $(g-2)$ [9], yields the total QED contribution $a_\mu(\mathrm{QED}) = 116\,584\,705.7(1.8)(0.5) \times 10^{-11}$ [11].

The hadronic contribution to $(g-2)$ cannot be calculated directly, but must be determined from data. The first-order hadronic vacuum polarization dominates the uncertainty in the theoretical value of a_μ, because it is calculated using dispersion theory and data from $e^+e^- \to$ hadrons and hadronic τ decay as input. The various order hadronic contributions are shown in Fig. 2. Diagrams for hadroproduction and hadronic τ decay are shown in Fig. 3. The most precise determination of the first-order hadronic contribution is [12] $a_\mu(\mathrm{had};1) = 6924(62) \times 10^{-11}$, which is 59.39 ± 0.53 ppm of a_μ, but there is continuing discussion of the use of CVC and the τ-decay data [13]. The higher-order contribution is [14] $a_\mu(\mathrm{had};2) = -101(6) \times 10^{-11}$. The hadronic light-by-light scattering shown in Fig. 4 has now been calculated by two groups [15, 16], using essentially the same model, and agreement is found: $a_\mu(\mathrm{had};\mathrm{lbl}) = -85(32)10^{-11}$. However, the two groups disagree on the uncertainty on the calculation, and I have taken the larger error from [16]. The uncertainty in this contribution could be reduced substantially by the appropriate calculation on the lattice, and perhaps by other additional calculations as well [17].

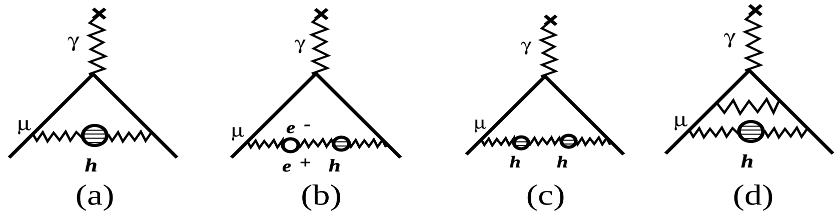

Figure 2: (a) The lowest-order hadronic contribution. (b-d) Higher-order hadronic contributions except for the light-by-light scattering contribution.

Figure 3: (a). The hadroproduction process which enters the dispersion relation. (b) Hadronic τ decay.

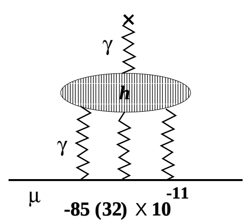

Figure 4: (a). The hadronic light-by-light scattering contribution.

The total hadronic contribution is given by $a_\mu(\text{had}; 1 + 2 + \text{lbl}) = 6738(70) \times 10^{-11}$ which is 57.79 ± 0.60 ppm of a_μ, with an uncertainty dominated by the uncertainty on the first-order hadronic vacuum polarization. It is precisely this contribution which is being addressed by the programs to measure $R(s)$ at BES and the Budker Institute [18]. We look forward to additional high quality data from these experiments and from DAPHNE [19], as well as τ-decay data from CLEO, to further reduce the uncertainty on the hadronic contribution.

The Standard Model electroweak contribution arises from the diagrams shown in Fig. 5. The Standard Model Higgs contribution is negligible. The single-loop

W and Z contributions were calculated by a number of authors shortly after the Standard Model was developed [20, 21, 22, 23]. The result is $a_\mu(\text{weak}; 1) = 195 \times 10^{-11}$ or 1.7 ppm of a_μ. Partial calculations [24, 25] of the two-loop electroweak contributions indicated that they might not be small. The full calculation [26, 27] which was later confirmed independently [28] showed that the total first- and second-order weak contribution was 20% less than the first-order result. The result is $a_\mu(\text{weak}; 1 + 2) = 151(4) \times 10^{-11}$, which is 1.30 ± 0.03 ppm of a_μ.

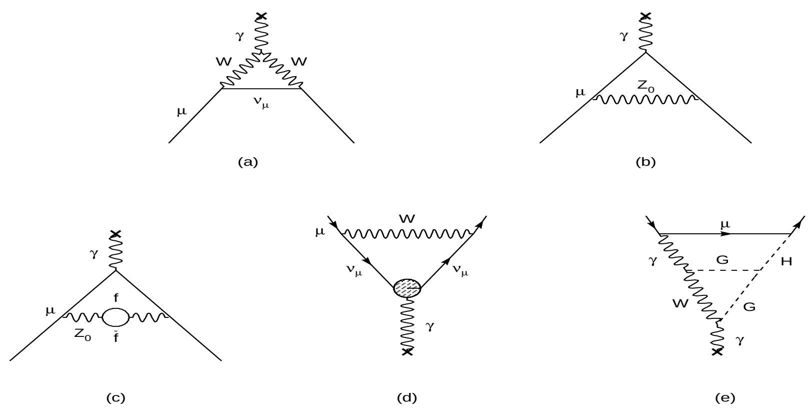

Figure 5: (a,b). The single-loop electroweak contributions. (The standard Higgs contribution is negligible.) (c-e) Examples of the higher-order electroweak contributions. (See [26, 27].)

The Standard Model prediction for a_μ is $a_\mu(\text{SM}) = (116\,591\,594.7{\pm}70){\times}10^{-11}$ ($\pm$0.60 ppm).

A great deal has been written about the possible contribution to the muon $(g-2)$ value from non-Standard Model physics. Just as the proton substructure produces a g-value which is not equal to two, muon substructure would also contribute to the anomalous moment, the critical issue being the scale of the substructure [29]. A Standard Model value for $(g-2)$ at the 0.35 ppm level would restrict the substructure scale to around 5 TeV.

In Fig. 5(a) the triple gauge vertex $WW\gamma$ appears, and it is through this diagram that the muon $(g-2)$ obtains its sensitivity to W substructure and anomalous gauge couplings. The combined sensitivity of LEP1, LEP2, and $(g-2)$, and the unique contribution which $(g-2)$ makes in constraining the existence of such couplings, is described by Renard *et al.* [30].

Supersymmetry has become a serious candidate for physics beyond the Standard Model. The SUSY contribution is shown in Fig. 6. In the case of large $\tan\beta$, the chargino diagram dominates and the contribution to $(g-2)$ from SUSY is

Figure 6: The lowest-order supersymmetric contributions to $(g-2)$.

given by [31]

$$a_\mu(\mathrm{SUSY}) \simeq \frac{\alpha}{8\pi \sin^2\theta_W}\frac{m_\mu^2}{\tilde{m}^2}\tan\beta \simeq 140\times 10^{-11}\ (\frac{100\ \mathrm{GeV}}{\tilde{m}})^2 \tan\beta. \qquad (3)$$

The goal of E821 is to reach a precision of $\pm 40\times 10^{-11}$ (± 0.35 ppm), so the factor of 140 above corresponds to 1.2 ppm. For $\tilde{m} = 750$ GeV and $\tan\beta = 40$, $a_\mu(\mathrm{SUSY}) = 100\times 10^{-11}$.

3 The New $(g - 2)$ Experiment

For polarized muons moving in a uniform magnetic field $\vec{B}$ which is perpendicular to the muon spin direction and to the plane of the orbit, and with an electric quadrupole field $\vec{E}$ for vertical focusing [10], the difference angular frequency, ω_a, between the spin precession frequency ω_s and the cyclotron frequency ω_c, is given by

$$\vec{\omega}_a = -\frac{e}{m}\left[a_\mu\vec{B} - \left(a_\mu - \frac{1}{\gamma^2-1}\right)\vec{\beta}\times\vec{E}\right]. \qquad (4)$$

The dependence of ω_a on the electric field is eliminated by storing muons with the “magic” γ_μ=29.3, which corresponds to a muon momentum $p_\mu = 3.09$ GeV/c. Hence measurement of ω_a and of B determines a_μ. At the magic gamma, the muon lifetime is $\gamma\tau = 64.4\ \mu$s, the $(g-2)$ precession period is 4.37 μs, and for the central orbit radius of 7.11 m the cyclotron period is 149 ns.

The storage ring magnet is a superferric 700 ton, 14 m diameter circular “C”-magnet, with the opening facing inward towards the ring center. The field is excited by three 14 m diameter superconducting coils which carry 5.2 kA from a low voltage power supply to produce the 1.45 T magnetic field [32]. The short term field stability over several AGS cycles is better than 0.1 ppm.

The magnetic field which enters in Eq. (4) is the average field seen by the muon distribution. Because direct injection of muons does not uniformly fill the phase space, we used a tracking code to calculate the distribution of muons in the storage ring. The radial distribution obtained from this tracking code was compared with the distribution obtained from observing the beam debunching in the ring at early times. The two distributions agreed quite well. In the 1999 run, a straw-tube array at one detector location provided information on the decay positron trajectories coming out of the storage region. These data will permit us to reconstruct directly the muon spatial distribution in one section of the ring.

In 1998, direct muon injection into the storage ring was employed for the first time. The AGS performance, the beamline and the inflector magnet [33] were as described in [34], and except for the muon injection, many of the experimental details are the same as described there. The positive muon beam with the magic momentum is formed by collecting the highest energy muons from pion decay in a 72 m long decay section of our beamline, which results in a muon polarization of 96%. The flux incident on the inflector magnet was 2×10^6 per fill of the ring.

The 10 mrad kick needed to put the muon beam onto a stable orbit was achieved with a current, because usual magnetic kicker techniques would spoil the precision magnetic field. Three pulse-forming networks powered three identical 1.7 m long kicker sections consisting of parallel plates on either side of the beam. Current flowed down one side, crossed over, and flowed back up the other side. The kicker plate geometry and composition was chosen to minimize eddy currents, and the eddy current effect on the total field seen by the muons was less than 0.1 ppm 20 μs after injection. The current pulse, which was formed by an under-damped LCR circuit, had a peak current of 4100 A and a pulse base width of 400 ns. Because the cyclotron period of the muon beam from the AGS was 149 ns, the beam was kicked several times before the kicker pulse died out. With muon injection, the number of detected positrons per hour was increased by an order of magnitude over pion injection. Thus, the use of a muon beam an order of magnitude less intense than the pion beam resulted in a substantial increase in stored muons per fill of the ring, with the injection related background reduced by about a factor of 50.

Positrons from the in-flight decay $\mu^+ \to e^+\nu_e\overline{\nu}_\mu$ are detected with Pb-scintillating fiber calorimeters placed symmetrically at 24 positions around the inside of the storage ring [35]. The decay positron time spectrum is [10, 36]

$$N_0 e^{-t/\gamma\tau}\left[1 + A(E)\cos\left(\omega_a t + \phi(E)\right)\right]. \tag{5}$$

The normalization constant N_0 and the parity violating asymmetry parameter $A(E)$ depend on the energy threshold placed on the positrons. The fractional statistical error on ω_a is proportional to $A^{-1}N_e^{-1/2}$, where N_e is the number of decay positrons detected above some energy threshold. For an energy threshold of 1.8 GeV, we measure A to be 0.34 consistent with its theoretical value [36], which we attribute to the good calorimeter energy resolution (σ/E = 10% at 1

GeV) and a scalloped vacuum chamber which minimizes pre-showering before the positrons reach the calorimeters.

The photomultiplier tubes of the calorimeter were gated off before injection and when gated on, they recovered to 90% pulse height in $\leq$ 400 ns, and reached full operating gain in several μs. With the reduced flash following injection, it was possible to begin counting as soon as 5 μs after injection in the region of the ring 180° around from the injection point.

The calorimeter pulses were continuously sampled by custom 400 MHz waveform digitizers (WFDs), which provided both timing and energy information for the positrons. Both the NMR and WFD clocks were phase-locked to the same LORAN-C frequency signal. The waveforms were zero-suppressed, and stored in memory in the WFD until the end of the AGS cycle. Between AGS acceleration cycles, the WFD data were written to tape for off-line analysis, as were the calorimeter calibration data and the magnetic field data.

A laser/LED calibration system was used to monitor calorimeter time and gain shifts during the data-collection period. Early-to-late timing shifts during the first 200 μs were on-average less than 20 ps, which is needed to keep systematic timing errors smaller than 0.1 ppm.

For the offline analysis, the detector response (waveform shape) to positrons was determined from our data for each calorimeter. These shapes were then fit to all pulses in the data to determine a time, an amplitude, and a width parameter for each pulse. Time histograms were formed for each detector. These independent data sets were analyzed separately and were in agreement ($\chi^2/\nu = 17.2/20$).

A completely blind analysis was performed on the data. Arbitrary offsets were put on the muon frequency and the proton frequency from the NMR probes. Each offset was known by one person, making it impossible to determine the actual value of a_μ. Only when the analysis of both the magnetic field and ω_a were completed were the offsets removed and the new value of a_μ determined.

After the offsets were removed, it was necessary to make two corrections to the frequency obtained from the fitting. For muons with the “magic” momentum, ω_a is not affected by the electric field. For the ensemble of muons in our storage ring there is a small electric field correction to ω_a because not all muons are at the magic momentum. There is also a pitch correction because of the vertical betatron oscillations [10, 36]. The sum of these two corrections for these data is (0.9 ± 0.2) ppm.

The dominant systematic errors which were reported in our first measurement [34] have been completely eliminated. The remaining systematic errors are under study. With many of them approximated by upper limits, one obtains a total systematic error of $\leq$ 1 ppm, with the systematic error assigned to the magnetic field of 0.5 ppm. Because the study of systematic errors is a source of much continuing work, we have chosen not to present a detailed list at this time.

We do wish to note the substantial improvement in the magnetic field quality which has been obtained by additional shimming. In Fig. 7 we show the average magnetic field from the 1997 and 1998 runs. The field uniformity over the storage aperture in 1998 was almost an order of magnitude better than was obtained in the CERN experiment [10].

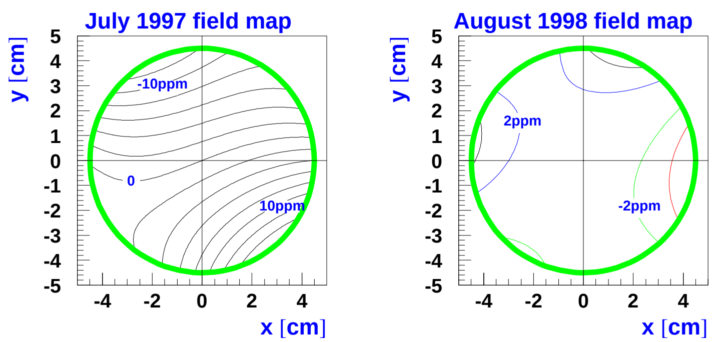

Figure 7: The magnetic field profile averaged over azimuth for July 1997 when the data reported [34] were taken, and for August 1998 when the new data reported here were taken. Each contour represents a 2 ppm change.

4 New Results

One month after the Symposium, we finished our analysis of the 1998 data and obtained a new result at the precision of ± 5 ppm [37].

Our experiment measures the frequency ratio $R = \omega_a/\omega_p$, where ω_p is the free proton NMR frequency in our magnetic field. Including the pitch and electric field corrections, we obtain $R = 3.707\ 201(19) \times 10^{-3}$, where the 5 ppm error includes a 1 ppm systematic error estimate. We obtain a_{μ^+} from $a_{\mu^+} = R/(\lambda - R)$ $= 116\ 591\ 91(59) \times 10^{-10}$ in which $\lambda = \mu_\mu/\mu_p = 3.183\ 345\ 39(10)$ [7, 38]. This new result is in good agreement with the mean of the CERN measurements for a_{μ^+} and a_{μ^-} [7], and our previous measurement of a_{μ^+} [34], which are tabulated below.

Assuming CPT symmetry, the weighted mean of the four measurements gives a new world average of $a_\mu = 116\ 592\ 10(46) \times 10^{-10}$ (± 3.9 ppm), which agrees with the Standard Model to within one standard deviation. These results are displayed graphically in Fig. 8. Also shown is the projected error from the 1999 data, and the ± 0.35 ppm goal of E821.

Measurement	*Value* $\times 10^{10}$
CERN [10] μ^+	116 591 03 (120) (10 ppm)
CERN [10] μ^-	116 593 65 (120) (10 ppm)
E821 [34] μ^+ π_{inj}	116 592 51 (150) (13 ppm)
E821 μ^+ μ_{inj}	116 591 91 (59) (5 ppm)
New World Average	116 592 10 (46) (4 ppm)

Table 1: The values of a_μ from the four most precise experiments. The new value for μ_μ/μ_p has been used to get a_μ from the measured ratio ω_a/ω_p. For the average, $\chi^2/\nu = 0.92$. The goal of the experiment is an error of ±4.0 in the units above. The fourth line is our new, and still preliminary, result [37].

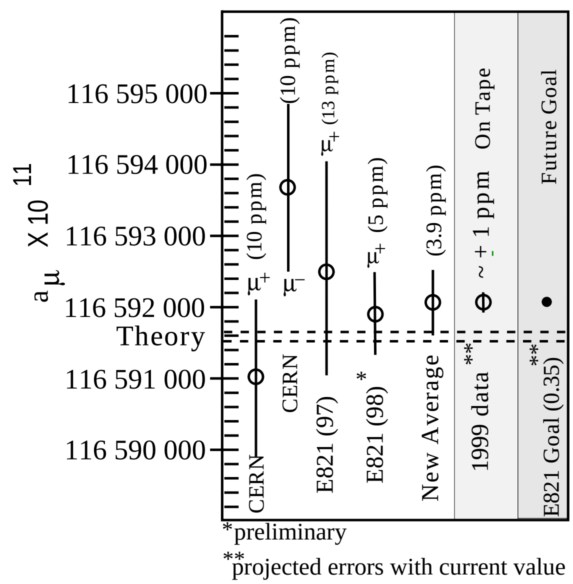

Figure 8: The four precise measurements of a_μ and the Standard Model value. To show the potential improvement available, the projected errors of 1 ppm and 0.35 ppm are shown on the right hand side with the central value equal to the present world average.

5 Outlook and Conclusions

The Standard Model has been remarkably successful in describing a wide range of phenomena including the entire body of results from LEP. The new result from E821, which has a precision of 5 parts per million, lowers the uncertainty on our knowledge of $(g-2)_\mu$ to 3.9 ppm. At that level, there is good agreement with the

Standard Model, but there is still room for the observation of a value at the level of one ppm or better which could agree with the previous measurements, and disagree with the Standard Model. We expect our one ppm result to be available before the end of 2000.

This experiment is very much a work in progress. The initial design of E821 was made with the systematic error budget of 0.12 ppm. Many of the improvements which were made to the CERN technique have indeed worked, making it straightforward to obtain a systematic error less than one ppm. While we have been learning about our systematic errors from the beginning of the first pion injection run, with the sub-ppm statistics available with muon injection we are now challenged to push the analysis of systematic errors to the limit. Our ultimate goal is a statistical answer at the 0.3 ppm level, with systematic errors at perhaps half this level. Our work thus far seems to indicate that this level of systematic error will be possible.

A new inflector magnet has been installed in the ring, which has a fringe field in the storage region a factor of 5 less than the old inflector had. This will improve our ability to map the field everywhere and will help to reduce the uncertainty on our knowledge of the field. The principal magnetic field issue remaining is our ability to track the field with time, and to understand the full calibration of the NMR probes to a few tenths of a ppm.

The other principal challenge is how to handle pile-up in the detectors without discarding an unreasonable portion of the data set. The dominant analysis effort now is to understand this effect.

It has been 20 years since the CERN experiment presented its final report which verified the hadronic contribution at the eight standard deviation level, but which left it to a future experiment to verify the electroweak contribution. The new Brookhaven experiment is now approaching that goal. Within the next few years either the Standard Model value will be confirmed, or evidence of a new contribution to the muon $(g-2)$ will be discovered.

I wish to acknowledge the efforts of the many collaborators who have worked on $(g-2)$ during the past 15 years. The steady support of the funding agencies (U.S. and abroad) and the Brookhaven Laboratory management was essential to our reaching this point. I wish to thank R. Carey, D. Hertzog, K. Jungmann, V. Hughes, J. Miller, Y. Semertzidis, and E. Sichtermann for their comments on this manuscript.

References

[1] The (g − 2) Collaboration consists of: R. M. Carey, W. Earle, E. Efstathiadis, E. S. Hazen, F. Krienen, I. Logashenko, J. P. Miller, J. Paley, O. Rind, B. L. Roberts, L. R. Sulak, A. Trofimov (Boston University), H. N. Brown, G. Bunce, G. T. Danby, R. Larsen, Y. Y. Lee, W. Meng, J. Mi, W.M. Morse, C. Özben, C. Pai, R. Prigl, R. Sanders, Y. Semertzidis, D. Warburton (Brookhaven National Laboratory), Y. Orlov (Cornell University), D. Winn (Fairfield University), A. Grossmann, K. Jungmann, G. zu Putlitz (University of Heidelberg), P. T. Debevec, W. Deninger, F. Gray, D. W. Hertzog, C. Onderwater, C. Polly, S. Sedykh, D. Urner (University of Illinois), U. Haeberlen (Max Planck Institute für Med. Forschung, Heidelberg), A. Yamamoto (KEK), P. Cushman, L. Duong, S. Giron, J. Kindem, R. McNabb, C. Timmermans, D. Zimmerman (University of Minnesota), V. P. Druzhinin, G. V. Fedotovich, B. I. Khazin, N. M. Ryskulov, Yu. M. Shatunov, E. Solodov (Budker Institute of Nuclear Physics, Novosibirsk), M. Iwasaki, M. Kawamura (Tokyo Institute of Technology), H. Deng, S.K. Dhawan, F.J.M. Farley, M. Grosse-Perdekamp, V. W. Hughes, D. Kawall, J. Pretz, S. I. Redin, A. Steinmetz (Yale University).

[2] O. Stern, Z. Phys. **7**, 18 (1921).

[3] W. Gerlach and O. Stern, Z. Phys. **8**, 110 (1922), Z. Phys. **9**, 349 (1922) and Z. Phys. **9**, 353 (1924).

[4] W. Gerlach and O. Stern, Ann. Phys. **74**, 45 (1924).

[5] J. E. Nafe, *et al.*, Phys. Rev. **71**, 914 (1947); D. E. Nagl, *et al.*, Phys. Rev. **72**, 971 (1947); P. Kusch and H.M. Foley, Phys. Rev. **74**, 250 (1948).

[6] J. Schwinger, Phys. Rev. **73**, 416 (1948), Phys. Rev. **75**, 898 (1949).

[7] Particle Data Group, Eur. Phys. J. C **3**, 1 (1998).

[8] R. S. Van Dyck *et al.*, PRL **59**, 26 (1987) and in Quantum Electrodynamics, (Directions in High Energy Physics Vol. 7) T. Kinoshita ed., World Scientific, 1990.

[9] T. Kinoshita, Rep. Prog. Phys. **59**, 1459 (1996).

[10] J. Bailey, *et al.*, Nucl. Phys. B **150**, 1 (1979).

[11] V. W. Hughes and T. Kinoshita, Rev. Mod. Phys. **71**, S133 (1999).

[12] M. Davier and A. Höcker, Phys. Lett. B **435**, 427 (1998) and references therein.

[13] S. I. Eidelman and V.N. Ivanchenko, Nucl. Phys. B (Proc. Suppl.) **76**, 319 (1999).

[14] B. Krause, Phys. Lett. B **390**, 392 (1997).

[15] M. Hayakawa and T. Kinoshita, Phys. Rev. D **57**, 465 (1998) and references therein.

[16] J. Bijnens, E. Pallante and J. Prades, Nucl. Phys. B **474**, 379 (1996) and references therein.

[17] E. de Rafael, private communication.

[18] Z.-G. Zhao, these proceedings.

[19] Sergio Bertolucci, these proceedings.

[20] W. A. Bardeen, R. Gastmans, and B Lautrup, Nucl. Phys. B **46**, 319 (1972).

[21] R. Jackiw and S. Weinberg, Phys. Rev. D **5**, 157 (1972).

[22] I. Bars and M. Yoshimura, Phys. Rev. D **6**, 374 (1972).

[23] J. Calmet, S. Narison, M. Perrottet, and E. De Rafael, Rev. Mod. Phys. **49**, 21 (1977).

[24] T. V. Kukhto, E. A. Kuraev, A. Schiller, and Z. K. Silagadze, Nucl. Phys. B **371**, 567 (1992).

[25] S. Peris, M. Perrottet, E. de Rafael, Phys. Lett. B **355**, 523 (1995).

[26] A. Czarnecki, B. Krause, and W. J. Marciano, Phys. Rev. D **52**, R2619 (1995).

[27] A. Czarnecki, B. Krause, and W. J. Marciano, Phys. Rev. Lett. **76**, 3267 (1996).

[28] G. Degrassi and G. F. Giudice, Phys. Rev. D **58**, 53007 (1998).

[29] An overview of non-Standard Model physics is given by T. Kinoshita and W. J. Marciano in Quantum Electrodynamics (Directions in High Energy Physics, Vol. 7), ed. T. Kinoshita, (World Scientific, Singapore, 1990), p. 419.

[30] F. Renard, *et al.*, Phys. Lett. B **409**, 398 (1997).

[31] A. Czarnecki and W. Marciano, Nucl. Phys. B (Proc. Suppl.) **76**, 245 (1999).

[32] G. T. Danby, *et al.*, in preparation, and G. T. Danby and J. W. Jackson, Proceedings of the 1987 IEEE Particle Accelerator Conference, ed. E.R. Lindstron and L.S. Taylor, (IEEE, 1987) p. 1517.

[33] F. Krienen, D. Loombah and W. Meng, Nucl. Inst. and Meth. A **283**, 5 (1989).

[34] R. M. Carey *et al.*, Phys. Rev. Lett. **82**, 1632 (1999).

[35] S. Sedykh *et al.*, Proceedings of the VII Int. Conf. on Calorimetry in High-Energy Physics (CALOR 97), ed. E. Cheu, T. Embry, J. Rutherfordh and R. Wigmans, World Scientific (1998), p. 269.

[36] F.J.M. Farley and E. Picasso in Quantum Electrodynamics, ed. T. Kinoshita, (World Scientific, Singapore, 1990), p. 479.

[37] $g-2$ Collaboration, http://www.phy.bnl.gov/g2muon/home.html.

[38] W. Liu, *et al.*, Phys. Rev. Lett. **82**, 711 (1999).